

Global versus Local Aromaticity in Porphyrinoid Macrocycles: Experimental and Theoretical Study of “Imidacene”, an Imidazole-Containing Analogue of Porphycene

Andrew L. Sargent,^{*[a]} Ian C. Hawkins,^[a] William E. Allen,^{*[a]} Hong Liu,^[a] Jonathan L. Sessler,^{*[b]} and Christopher J. Fowler^[b]

Abstract: The synthesis, spectroscopic properties, and computational analysis of an imidazole-based analogue of porphycene are described. The macrocycle, given the trivial name “imidacene”, was prepared by reductive coupling of a diformyl-substituted 2,2'-biimidazole using low-valent titanium, followed by treatment with 2,3-dichloro-5,6-dicyano-1,4-benzoquinone. Imidacene displays a porphyrin-like electronic structure, as judged by its ¹H NMR, ¹³C NMR, and UV/Vis spectral characteristics. Despite a cyclic 18 π -electron pathway, dichloromethane or ethyl acetate solutions of imidacene were found to undergo rapid decomposition, even in the

absence of light and air. A series of high-level theoretical calculations, performed to probe the origin of this instability, revealed that the presence of a delocalized 18 π -electron pathway in both imidacene and porphycene provides less aromatic stabilization energy than locally aromatic 6 π -electron heterocycles in their reduced counterparts. That reduction of imidacene occurs on perimeter nitrogen atoms allows it to maintain its planarity and two stabilizing

intramolecular hydrogen bonds, thereby distinguishing it from porphycene and, more generally, from porphyrin. Despite the presence of both 18 π - and 22 π -electron pathways in the planar, reduced form of imidacene, aromaticity is evident only in the 6 π -electron five-membered rings. Our computational analysis predicts that routine ¹H NMR spectroscopy can be used to distinguish between local and global aromaticity in planar porphyrinoid macrocycles; the difference in the chemical shift for the internal *NH* protons is expected to be on the order of 19 ppm for these two electronically disparate sets of ostensibly similar compounds.

Keywords: ab initio calculations • annulenes • aromaticity • biimidazoles • porphyrinoids

Introduction

Porphyrin contains an 18 π -electron pathway and has long been considered a quintessential aromatic system. To probe the limits of large-scale electron delocalization, numerous structural isomers of porphyrin, and derivatives containing heteroatoms other than nitrogen, have been synthesized.^[1] The consensus impression that has emerged from these studies is that Nature's recipe for porphyrinoid aromaticity—four heterocycles connected by various combinations of direct linkages or sp² hybridized bridging groups—is quite

forgiving, provided that a planar array containing a $4n+2$ π -electron conjugation pathway can be accommodated. Among the ever-increasing number of polypyrrole macrocycles that cannot become “globally” aromatic are the so-called calixpyrroles and calixphyrins,^[2] which are stable toward oxidation because they lack hydrogen atoms on the *meso* carbons, and expanded porphyrins that are incapable of assuming a flat geometry.^[3] Although non-planar globally aromatic porphyrinoid systems are known,^[4] the π -orbital overlap and, hence, the electron delocalization, is maximized in planar structures.

Computational approaches to the study of aromaticity^[5] and, in particular, the delineation of large molecules into locally and globally aromatic regions, include the calculation of aromatic stabilization energies (ASEs)^[6] or resonance energies (RE);^[7] these have been recently upstaged by methods that use the harmonic oscillator model of aromaticity (HOMA),^[8] nucleus independent chemical shifts (NICS),^[9] and the continuous transformation of origin of current densities (CTOCD),^[10] Chemical systems ranging from fullerenes^[11] to benzocyclynes^[12] have been analyzed to determine the extent of global versus local aromaticity, and these studies have been motivated, in large part, by the desire to

[a] Dr. A. L. Sargent, Prof. Dr. W. E. Allen, I. C. Hawkins, H. Liu
Department of Chemistry, East Carolina University
Greenville, NC 27858-4353 (USA)
Fax: (+1) 252-328-6210
E-mail: allenwi@mail.ecu.edu
sargenta@mail.ecu.edu

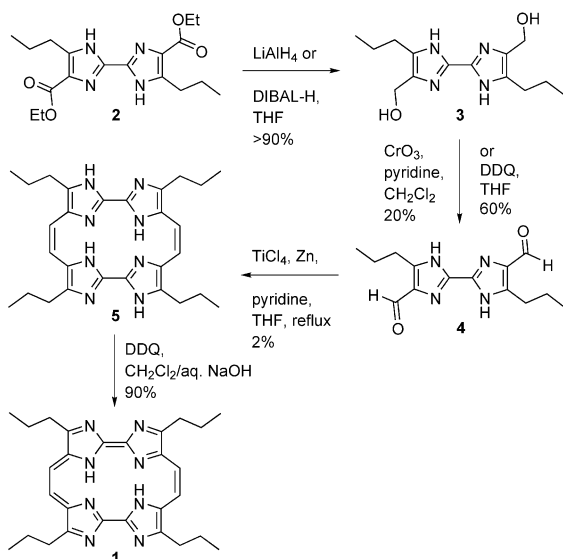
[b] Prof. Dr. J. L. Sessler, Dr. C. J. Fowler
Department of Chemistry and Biochemistry
Institute for Cellular and Molecular Biology
The University of Texas at Austin
Austin, TX 78712-1167 (USA)
E-mail: sessler@mail.utexas.edu

understand the chemical properties and reactivity associated with the two classifications. In this paper we bring a combination of approaches to bear upon a newly synthesized porphyrin-like molecule that displays unexpectedly low stability, in spite of the presence of a formal $4n+2$ π -electron pathway.

The molecule that motivated this study is the imidazole-containing macrocycle **1**, to which we have given the trivial name "imidacene" in order to highlight its structural similarity to porphycene. Our efforts attempt to answer several questions, including: how can imidacene (**1**) and porphycene (**Pc**), two very closely related macrocycles, exhibit opposite relative stabilities with respect to their reduced counterparts? Additionally, how can the precursor to **1**, "dihydroimidacene" (**5**), which formally possesses both 18- and 22 π -electron pathways, display none of the spectral characteristics of a globally aromatic porphyrinoid?

Results and Discussion

Synthesis: In analogy to the procedure used to prepare various porphyrin isomers and expanded porphyrins, preparation of imidazole-based porphyrinoids was expected to proceed via a biimidazole dialdehyde. Following a strategy similar to the one used to prepare porphycene,^[13] it was expected that Ti-mediated dicarbonyl coupling of two biimidazole molecules would install the bridging CH=CH units of the macrocycle. Thus, initial work focused on converting the known biimidazole diester **2**^[14] to the corresponding dialdehyde **4** (Scheme 1). Treatment of **2** with DIBAL-H in CH₂Cl₂ at -78°C was ineffective; only a diol (from over-reduction)



Scheme 1.

and unchanged diester **2** could be detected in the reaction mixture. The failure to effect the direct transformation of **2** to the desired diformyl intermediate **4** forced us to pursue a more lengthy ester \rightarrow alcohol \rightarrow aldehyde conversion sequence. In pursuing this strategy, it was found that diol **3** was produced in 92% yield by treatment of **2** with LiAlH₄ in THF

for 3 d at RT. Efforts to increase the rate of this reaction by heating at reflux caused complete deoxygenation of the biimidazole, giving rise to the corresponding dimethyl derivative.^[14] Thus, a more optimal set of conditions was sought and, in due course, it was found that **3** could be produced in almost quantitative yield in 2 h by treating **2** with DIBAL-H in THF at reflux.

Oxidation of diol **3** to the corresponding dialdehyde **4** could be effected in low yield (20%) by using Collins's reagent (prepared in situ in CH₂Cl₂), or in up to 60% yield by treating **3** with 2,3-dichloro-5,6-dicyano-1,4-benzoquinone (DDQ) in THF. The low yield of the former procedure arose from over-oxidation of the initially formed, highly soluble aldehyde(s) to carboxylic acid(s) during the long reaction time required for complete consumption of **3**. Other oxidation attempts, including the use of MnO₂ or Swern conditions (DMSO, (COCl)₂, Et₃N), were unsuccessful.

With the requisite macrocycle precursor **4** in hand, a model Ti-promoted carbonyl coupling reaction was run using a simple commercially available carbonyl-containing imidazole, namely 5-methyl-4-imidazolecarboxaldehyde. Specifically, TiCl₄/Zn was used to generate a low-valent titanium reagent, at which point the imidazole aldehyde was added to the reaction vessel. Under these reaction conditions, the expected *trans*-alkene product was obtained in 54% yield, along with 14% of the *cis* isomer. The use of this protocol, but under conditions of high dilution, then afforded the tetrapropyl-dihydroimidacene (**5**) as a yellow solid in $\approx 2\%$ yield.^[15] As the *trans* intermediate is presumably dominant along the reaction pathway, the yield of macrocycle (generated from the *cis* species only) is very low. However, **5** is the only nonpolymeric compound produced under the reaction conditions. It was thus readily purified by column chromatography over silica gel.

In the preparation of porphycene, the presumed [20]annulene intermediate **H₂Pc** is so susceptible to autoxidation that it escapes detection even when oxygen is excluded from the McMurry reaction medium.^[1c] In contrast, macrocycle **5** does not undergo spontaneous two-electron oxidation under the Ti-coupling conditions. During subsequent workup, however, traces of oxidized material can be observed by TLC as a spot which is blue under ordinary room light. Compound **5** was found to be indefinitely stable in the solid state, and has been stored in CH₂Cl₂ or EtOAc solution for months under anaerobic conditions.

In our case, treatment with strong oxidants {such as DDQ or [Mn^{III}(acac)₃] } is required to effect complete oxidation. Addition of such oxidants to yellow solutions of dihydroimidacene **5** in CH₂Cl₂ caused them to turn dark blue immediately, a change that was considered to reflect the formation of imidacene (**1**). When DDQ was used as the oxidant, **1** was obtained in 90% yield after column chromatography. Bubbling O₂ into CH₂Cl₂ or EtOAc solutions of **5** for one week does not effect complete oxidation, as judged by the fact that they retain a persistent green color.

Spectroscopy: In CDCl₃, the room-temperature ¹H NMR spectrum of dihydroimidacene (**5**) displays only five sets of peaks when scanned from 12 to -2 ppm: three from the hydrogens of the propyl groups, a singlet at 5.86 ppm assigned

to the bridging $CH=CH$ fragments, and a very broad singlet centered about 8.3 ppm ascribed to the NH protons. (The NH protons readily exchange with adventitious H_2O , as judged by their overly large integral value ($>6H$.) The simplicity of this spectrum suggests that rapid NH tautomerism takes place on the NMR time-scale. Dihydroimidacene is clearly not globally aromatic, as the singlet at 5.86 ppm is similar to those of the corresponding vinylic protons in simple^[16] and bridged macrocyclic $[4n]$ annulenes.^[17] Complementary to the 1H NMR spectrum, seven signals occur in the ^{13}C NMR spectrum; the resonance at 113.8 ppm is assigned to the sp^2 -hybridized carbon atoms of the $CH=CH$ bridges.

The 1H NMR spectrum of **1** is consistent with its presumed global aromaticity. All of the protons, except those of the NH groups, experience pronounced downfield shifts. Protons H-9, 10, 19, and 20 of the imidacene skeleton appear as a singlet at low field ($\delta=9.53$ ppm, i.e., at a chemical shift typical for bridging methine units of porphyrins). The NH protons of normal porphyrins typically appear upfield from TMS (-2 to -4 ppm). However, no peaks were observed in this region of the spectrum for **1**. Instead, a broad singlet at 2.02 ppm is tentatively ascribed to these hydrogen atoms (see below). For comparison, the inner NH atoms of tetrapropylporphycene resonate at about 3.0 ppm.^[13] In the ^{13}C NMR spectrum of **1**, like in that of **5**, seven signals are observed. One of the carbon atoms of the imidazole rings exhibits an unusual deviation, undergoing a downfield shift from about 140 to 172 ppm, while the other quaternary carbons are observed in the typical aromatic region (≈ 140 ppm, similar to those in **2–5**) (see below).

The electronic absorption spectrum of **1** in CH_2Cl_2 is also consistent with a globally aromatic, porphyrin-like 18π -electron compound. It consists of a Soret-like band at $\lambda=373$ nm ($\epsilon=130000$), a shoulder at 380 nm, and three longer-wavelength Q-type bands at $\lambda=611$ (49000), 645 (59000), and 686 nm (77000) (Figure 1). This absorption pattern resembles

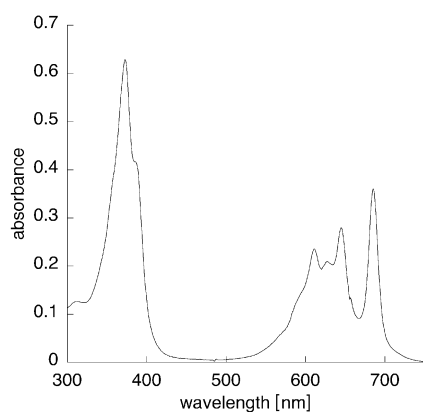


Figure 1. Electronic absorption spectrum of **1** (6.1×10^{-6} M) in CH_2Cl_2 .

that of tetrapropylporphycene^[13] (in CH_2Cl_2 , $\lambda=370$ ($\epsilon=142000$), 381 (100200), 560 (36400), 600 (34100), 633 nm (48200)). However, the Q bands of imidacene (**1**) are more intense and are red-shifted by about 50 nm relative to those of tetrapropylporphycene. According to the perimeter model,^[4, 18] a relatively large Q/Soret intensity ratio, coupled with a large splitting between the two components of the LUMO

pair, are characteristics of so-called “negative-hard” chromophores like porphycene. Given the similarities in structure, **1** would be expected to fall under this class as well. For solutions of **5** in either CH_2Cl_2 or CH_3CN , no peaks are observed from 400–800 nm, indicative of its lack of porphyrinoid aromaticity. Furthermore, its absorption bands in the higher-energy region of the spectrum are almost an order of magnitude less intense than typical Soret bands.

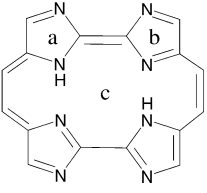
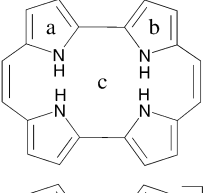
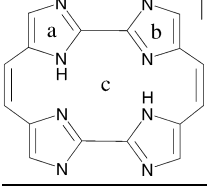
Once formed, **1** does not display the characteristic stability of porphyrins. For example, spectroscopic studies have shown that imidacene is very sensitive to acid. Upon treatment with 1 μ L of neat CF_3COOH , a blue sample of **1** in CH_2Cl_2 (3.0 mL of a 6×10^{-6} M solution) turns yellow within 30 s. The Q bands completely disappear, indicating that the resulting decomposition product(s) do not retain a porphyrin-like electronic structure. Furthermore, in the absence of acid, nitrogen-purged CH_2Cl_2 solutions of **1** slowly turn from blue to green, even when they are excluded from light. The unexpected low chemical stability of **1** prompted us to examine its properties (and those of its precursor **5**) using computational methods. To put the results in context, we applied the same theoretical treatments to other porphyrinoids, as described below.

Theoretical analysis: Three criteria for defining aromaticity were utilized with the understanding that each has known limitations which prevent its use as the sole criterion for making comprehensive characterizations.^[6a] In this context, the three criteria were evaluated to provide a measure of self-consistency and were based on 1) energetics, 2) magnetic properties, and 3) structural properties. Details of the three methods are described in the Experimental Section.

The data listed in Table 1 support the contention that locally aromatic porphyrinoid macrocycles possess more resonance stabilization energy (i.e., larger ASEs) than their globally aromatic counterparts. In the absence of other overriding energetic factors such as stabilizing hydrogen bonding or destabilizing steric crowding, the larger ASE may favor the reduced, or locally aromatic, form of the macrocycle (e.g., **5**). In porphycene and porphyrin, this is not the case as the reduced form of the macrocycle is energetically destabilized by steric crowding and a loss of $N-H \cdots N$ bonding in the binding pocket. Imidacene **1**, however, is unique in this regard. Reduction of **1** occurs at the exocyclic, perimeter N atoms, enabling both the oxidized and reduced forms of the macrocycle to be sterically unencumbered and maintain not only planarity but also the two strong $N-H \cdots N$ bonds in the binding pocket. Assuming that planarity, sterics, and hydrogen bonding play an important role in the stability of the molecule, compounds **1** and **5** provide a unique “matched set” with which to assess the contributions of local and global aromaticity. Since, in the gas phase, both oxidized and reduced species are planar, have two stabilizing intramolecular hydrogen bonds, and possess at least two locally aromatic five-membered rings, the relative stabilities are likely governed by additional local or global aromaticity.

The NICS and HOMA values listed in Table 1 for the various molecules clarify which rings within the macrocycles are aromatic. The values support the assertion that imidacene **1** and porphycene **Pc** possess both local (6 π -electron) and

Table 1. Calculated ASEs [kcal mol⁻¹], NICS [ppm], and HOMA values for various porphyrinoid macrocycles.

Macrocycle	ASE ^[a]	NICS ^[b]	HOMA ^[c]		
	38.9	a: -12.91 -12.69 12.28 ^[d]	a: 0.820 0.819 0.769 ^[d]		
		b: -4.54 -4.81 -3.70 ^[d]	b: 0.659 0.666 0.573 ^[d]		
		c: -13.96 -13.73 -13.98 ^[d]	c: 0.909 0.911 0.911 ^[d]		
		a: -11.73 -11.73 -11.28 ^[d]	a: 0.942 0.942 0.921 ^[d]		
		b: -11.75 -11.71 -11.12 ^[d]	b: 0.900 0.900 0.883 ^[d]		
		c: +4.27 +4.44 +4.18 ^[d]	c: 0.556 0.558 0.567 ^[d]		
		a: -14.31 -14.09	a: 0.748 0.746		
		b: -5.85 -6.09	b: 0.518 0.527		
		c: -15.24 -15.05	c: 0.910 0.911		
		a: -10.39 -10.40	a: 0.836 0.839		
	88.4	b: -10.39 -10.40	b: 0.836 0.839		
		c: +5.44 +5.46	c: 0.487 0.488		
		a: -10.28 -10.27	a: 0.874 0.876		
		b: -10.32 -10.33	b: 0.857 0.859		
		c: +7.34 +7.48	c: 0.542 0.544		
		a: -10.09 -10.09 -10.15	a: 0.921 0.922 0.916		
		b: -10.01 -10.04 -10.13	b: 0.919 0.920 0.912		
		c: +5.72 +5.89 +5.90	c: 0.520 0.523 0.511		
			72.8	b: -10.01 -10.04 -10.13	b: 0.919 0.920 0.912
				c: +5.72 +5.89 +5.90	c: 0.520 0.523 0.511

[a] Computational level is B3LYP/6-31G. [b], [c] Computational level is GIAO-SCF/6-31+G**/B3LYP/6-31G*. Italicized values correspond to GIAO-SCF/6-31+G**/B3LYP/6-31G**. Bold values correspond to GIAO-SCF/6-31++G**/B3LYP/6-31+G**. [d] Correspond to tetrapropyl analogue. [e] The “all N-H in” tautomer of **5** is +37.38 kcal mol⁻¹ higher in energy, and thus its ASE was not evaluated.

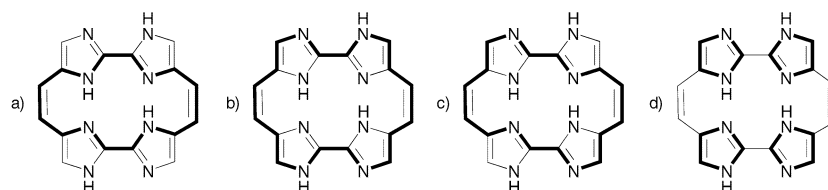


Figure 2. Possible π -electron delocalization pathways in dihydroimidacene **5**. a) 18 π -electron “internal cross”; b) 22 π -electron perimeter; c) 18 π -electron bridged [18]annulene; and d) 6 π -electron five-membered rings.

global (18 π -electron) aromatic pathways (rings “a” and “c”, respectively) while dihydroimidacene **5**, dihydroporphycene **H₂Pc** and the dianions of imidacene and porphycene possess only locally aromatic pathways (rings “a” and “b”). Interestingly, despite the presence of 18- and 22 π -electron pathways (Figure 2), macrocycle **5** is exclusively locally aromatic, in agreement with the experimental spectroscopic findings. Unlike typical porphyrinoid macrocycles, **5** possesses cyclic 6 π -, 18 π -, and 22 π -electron pathways, yet exhibits delocalization only among the 6 π -electron paths. Importantly, the NICS and HOMA values calculated with larger basis sets did not significantly alter the results.

That imidacene has a lower ASE than porphycene (38.9 vs 55.1 kcal mol⁻¹) is understandable in light of the fact that the ASE of imidazole is lower than that for pyrrole. The ASE of dihydroporphycene, however, is lower than that for dihydroimidacene (88.4 vs 91.5 kcal mol⁻¹) and may be a consequence of the geometric perturbation resulting from the steric congestion in the macrocyclic pocket and the consequent decrease in aromaticity. Although both the EN and GEO terms of HOMA for the pyrrole rings are smaller for dihydroporphycene (0.102, 0.062) than for porphycene (0.144, 0.108), indicating that the average bond length is closer to the optimal value and that there is less bond length alternation in dihydroporphycene, the steric repulsion within this molecule results in significant sp³ hybrid character at the nitrogen atoms. This, in turn, adversely affects the overlap of the two π electrons of the nitrogen atom with the π system of the ring and therefore yields a smaller ASE. The rigorously planar porphycene dianion does not suffer this fate and consequently exhibits a higher value of the ASE, relative to the corresponding imidacene dianion, as expected based on the higher ASEs of the constituent pyrrole rings.

The calculated ¹³C and ¹H NMR spectra for **1** and **5** are shown in Figures 3 and 4, respectively. Calculated chemical shifts of symmetry-equivalent nuclei were averaged to account for the facile N-H tautomerization within these molecules.^[19] For the ¹³C NMR data, agreement between the experimental and calculated chemical shifts is remarkable. In particular, theory correctly predicts that the ¹³C resonance of **1** at lowest field lies far outside the region of typical aromatic carbons ($\delta_{\text{exptl}} = 172.8$ ppm; $\delta_{\text{calcd}} = 176.7$ ppm). The experimental spectrum of tetrapropylporphycene, on the other hand, displays no resonances beyond 145 ppm. The unusual downfield signal of **1** arises from imine-like character at the imidazole carbons isolated from the 18 π -electron pathway of the “internal cross”^[20] (Figure 2a illustrates the internal cross for **5**).

For the calculated ¹H NMR spectra, it is important to note that inclusion of polarization functions on hydrogen impacts, as expected,^[21] the chemical shifts of the protons involved in

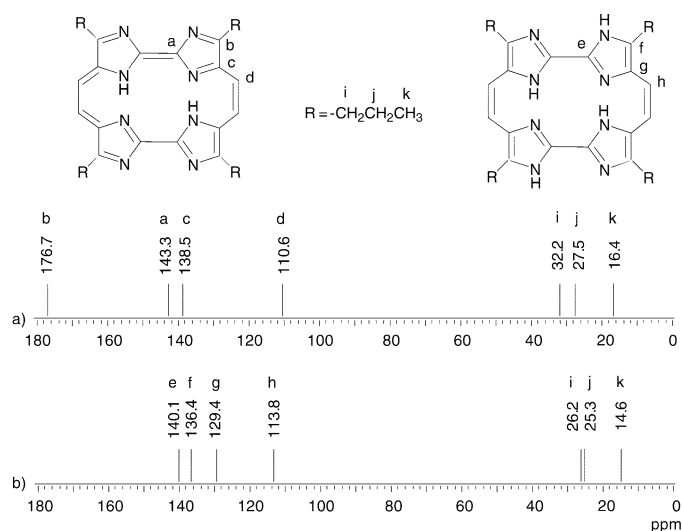


Figure 3. Simulated ^{13}C NMR spectrum of a) **1** and b) **5** calculated at the GIAO-SCF/6-31+G**/B3LYP/6-31G* level of theory.

hydrogen bonding. As shown in Figure 4b, the inner NH protons of imidacene are predicted to resonate at 1.17 ppm at this level of theory. The result is in reasonable agreement with our experimental assignment of the singlet at about 2.0 ppm. When hydrogen polarization functions are not included, the calculated chemical shift is predicted to be approximately -1.4 ppm (Figure 4a and c).

Of particular interest, our analysis predicts an unprecedented change in δ of approximately 19 ppm for the NH protons in the macrocyclic pocket upon reduction of imidacene. The result is understandable in terms of the opposite effect of local versus global ring currents on the internal NH protons. The global ring current induces a magnetic field that opposes the applied field at these protons, while the local ring currents induce magnetic fields that augment the applied field at these positions, as illustrated in Figure 5. Although the effect of ring currents from adjacent, locally aromatic rings is additive to a certain degree, it is the closed system of the macrocycle that results in the pronounced deshielding from the induced magnetic fields of

the individual rings. The difference in δ calculated for the NH proton in imidazole and a non-macrocyclic system such as biimidazole, for instance, is only 1.26 ppm ($\delta = 7.91, 9.17$ ppm for imidazole and biimidazole, respectively). Accounting for the influence of a total of four imidazoles therefore yields an overall chemical shift of $\delta = 11.69$ ppm for the inner NH protons, falling far short of the predicted $\delta = 19.49$ ppm for the corresponding locally aromatic macrocycle (Figure 4e).

Our calculations suggest that this effect is general for planar porphyrinoid macrocycles and that it serves as a fingerprint for either local or global aromaticity in these systems. The dianion of porphycene is known^[22] and calculations on this system predict that the NH protons will exhibit a large downfield chemical shift: neutral porphycene $\delta = -0.78$ ppm, porphycene dianion $\delta = 21.70$ ppm (yielding change in $\delta = 22.48$ ppm), at the GIAO-SCF/6-31+G**/B3LYP/6-31G** level of theory.

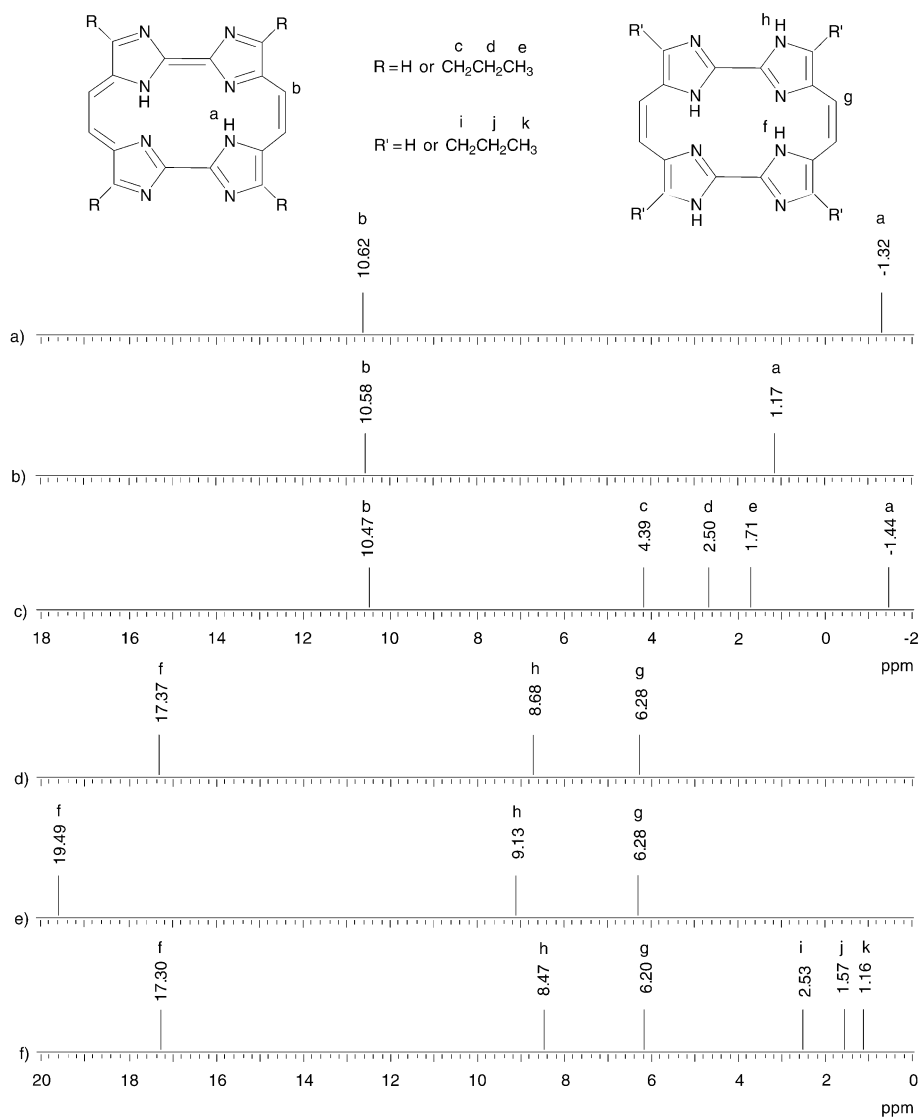


Figure 4. Simulated ^1H NMR spectrum of imidacene a) $\text{R} = \text{H}$, at GIAO-SCF/6-31+G**/B3LYP/6-31G*; b) $\text{R} = \text{H}$, at GIAO-SCF/6-31+G**/B3LYP/6-31G**; c) $\text{R} = \text{CH}_2\text{CH}_2\text{CH}_3$, at GIAO-SCF/6-31+G**/B3LYP/6-31G* and dihydroimidacene; d) $\text{R}' = \text{H}$, at GIAO-SCF/6-31+G**/B3LYP/6-31G*; e) $\text{R}' = \text{H}$, at GIAO-SCF/6-31+G**/B3LYP/6-31G**; f) $\text{R}' = \text{CH}_2\text{CH}_2\text{CH}_3$, at GIAO-SCF/6-31+G**/B3LYP/6-31G*.

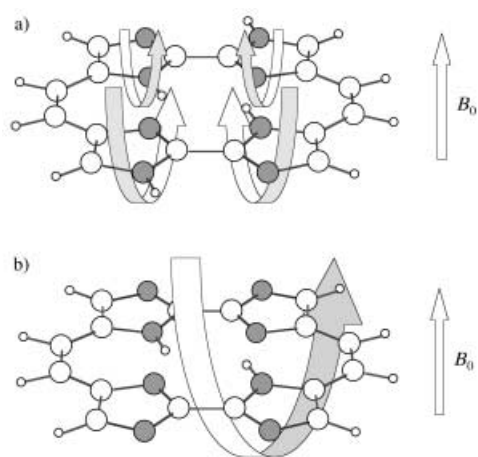


Figure 5. Effects of ring currents in an applied magnetic field for the a) locally aromatic **5** and b) globally aromatic **1**.

This dianion can be compared to the one produced by reduction of free base porphyrin. The latter species, which is not to be confused with the dianion produced by double deprotonation of porphyrin, is a tetraradical, with the unpaired electrons located on each of the four methyne bridges. As such, the locally aromatic molecule could possess a mixed spin-state with contributions from the singlet, triplet, and quintet states. Preliminary calculations suggest that the triplet is dominant, but that the quintet plays a significant role in the mixed spin-state system. Evaluation of the chemical shift for this system is not trivial, but calculations are in progress. To the extent that they can be predicted with reliability, a benefit of the present study will be a more complete understanding of the factors that regulate the electronic structure features of porphyrin-type systems and an improved ability to predict which among myriad possible target porphyrin analogue structures will display high chemical stability or interesting spectroscopic features. On a very different and more experimental level, this work leads to the prediction that conjugated macrocycles containing imidazole and biimidazole subunits may prove challenging to make but will surely display features very different from their pyrrole-containing analogues.

Experimental Section

(4'-Hydroxymethyl-5,5'-dipropyl-1*H*,1'*H*-[2,2']biimidazolyl-4-yl)-methanol (**3**)

Method A: Diester **2** (4.65 g, 12.8 mmol) was added slowly to a suspension of lithium aluminum hydride (95%, 1.82 g, 48.0 mmol) in dry THF (200 mL) at 0 °C. The reaction mixture was allowed to warm to RT. After 3 d, ice water was added dropwise until gas evolution ceased. The volatile components were removed by rotary evaporation to afford a slate-green solid. The solid was suspended in water (125 mL), and 10% aqueous HCl was added dropwise until the pH was 7–8. A light pink precipitate was removed by suction filtration and was washed with small portions of water. The filter cake was added to boiling CH₃OH (200 mL); this suspension was then filtered to remove insoluble salts. Evaporation of the filtrate provided diol **3** as a light pink solid (3.28 g, 92%).

Method B: DIBAL-H in toluene (1.0 M, 29 mL, 29.0 mmol) was added dropwise to a suspension of diester **2** (1.50 g, 4.14 mmol) in dry THF (50 mL) at 0 °C under N₂. After 30 min, the ice bath was removed and the

flask was heated to reflux for an additional 2 h. During this time, the reaction mixture became homogeneous. The mixture was cooled to 0 °C and the excess DIBAL-H was destroyed by dropwise addition of 10% HCl (5 mL) and H₂O (50 mL). After stirring for 2 h, the precipitate was removed by filtration through a layer of Celite. The Celite was washed with methanol (100 mL), and the filtrate was evaporated under reduced pressure. Saturated aqueous NaHCO₃ (20 mL) was added, and the suspension was magnetically stirred for 10 min. The white solid product was collected by filtration, washed with water, and dried to give diol **3** (1.13 g, 98%). ¹H NMR (CD₃OD): δ = 0.97 (t, 6H, CH₃CH₂CH₂), 1.70 (m, 4H, CH₃CH₂CH₂), 2.65 (t, 4H, CH₃CH₂CH₂), 4.54 (s, 4H, CH₂OH); ¹³C NMR (CD₃OD): δ = 14.2, 24.4, 28.0, 56.4, 134.7, 138.6.

5,5'-Dipropyl-1*H*,1'*H*-[2,2']biimidazolyl-4,4'-dicarbaldehyde (**4**)

Method A: Under N₂, CrO₃ (1.10 g, 10.8 mmol) was added to dry pyridine (1.75 g, 21.6 mmol) in dry CH₂Cl₂ (100 mL). The reaction mixture was stirred at RT for 30 min and was then cooled to 0 °C. Diol **3** (0.50 g, 1.8 mmol) was added in one portion at 0 °C. The ice bath was removed, and stirring was continued for 2 h. After passing the reaction mixture through a pad of silica gel and washing the pad with ethyl acetate (50 mL), the filtrate was washed with 2% NaOH (2 × 50 mL), then brine. The organic phase was dried over Na₂SO₄ and concentrated in vacuo. Flash chromatography over silica gel eluting with ethyl acetate gave dialdehyde **4** as a yellow solid (0.099 g, 20%).

Method B: Diol **3** (0.50 g, 1.8 mmol) and 2,3-dichloro-5,6-dicyano-1,4-benzoquinone (98%, 0.85 g, 3.67 mmol) were added to dry THF (80 mL), and the dark violet-black reaction was stirred for 48 h at RT. TLC analysis (silica gel, CHCl₃/CH₃OH 10:1) showed the presence of a new fast spot glowing blue under shortwave UV light. The mixture was diluted with ethyl acetate (150 mL), then was washed with 1% NaOH (4 × 25 mL) and brine. The NaOH solution was extracted with ethyl acetate (2 × 50 mL), and the combined organic layers were dried over MgSO₄ and concentrated by rotary evaporation. The crude product (a tan foam) was purified by flash chromatography over silica gel eluting with CHCl₃/CH₃OH 10:1 to afford compound **4** (0.30 g, 60%). ¹H NMR (CDCl₃): δ = 0.96 (t, 6H, CH₃CH₂CH₂), 1.73 (m, 4H, CH₃CH₂CH₂), 2.92 (t, 4H, CH₃CH₂CH₂), 9.82 (s, 2H, CHO); ¹³C NMR (CDCl₃): δ = 14.0, 23.5, 27.3, 137.1, 139.9, 146.4, 185.1; elemental analysis calcd (%) for C₁₄H₁₈N₄O₂ · ½ H₂O: C 60.80, H 6.65, N 20.26; found: C 60.80, H 6.64, N 20.25.

2,7,12,17-Tetrapropylidihydroimidacene (5): A flame-dried 500 mL three-necked round-bottomed flask was charged with Zn dust (3.65 g, 54.7 mmol), pyridine (1.0 mL), and dry THF (120 mL). The mixture was cooled to 0 °C under N₂, then TiCl₄ (3.0 mL, 27 mmol) was added dropwise. The resulting mixture was heated to reflux for 3 h. Dialdehyde **4** (0.50 g, 1.8 mmol) was added in one portion, and stirring was continued at reflux for an additional 4 h. The reaction was cooled to RT, and was filtered through a bed of Celite. The filter cake was washed with ethyl acetate. The filtrate was washed with 10% H₂SO₄ (2 × 100 mL) and brine; the aqueous layer was then extracted with ethyl acetate (2 × 150 mL). The combined organic layers were neutralized by adding 10% aqueous NaOH (80 mL) and stirring at RT for 30 min. Filtration through a bed of Celite removed a white precipitate that formed during neutralization. The filtrate was washed with brine and dried over Na₂SO₄. Filtration and flash column chromatography over silica gel using CHCl₃/CH₃OH 10:1 gave the product **5** as a yellow solid (10 mg, 2%). ¹H NMR (CDCl₃): δ = 0.93 (t, 12H, CH₃CH₂CH₂), 1.65 (m, 8H, CH₃CH₂CH₂), 2.56 (t, 8H, CH₃CH₂CH₂), 5.86 (s, 4H, CH=CH), 8.0–8.5 (brs, NH; exchanging with adventitious H₂O); ¹³C NMR (CDCl₃): δ = 14.1, 23.5, 27.3, 113.9, 132.1, 135.2, 137.2; elemental analysis calcd (%) for C₂₈H₃₆N₈ · (EtOAc) · 1.5 H₂O: C 64.08, H 7.90, N 18.68; found: C 63.92, H 7.84, N 18.86.

2,7,12,17-Tetrapropylimidacene (1): A separatory funnel was charged with a solution of dihydroimidacene **5** (10 mg, 0.021 mmol) in CH₂Cl₂ (100 mL), and a solution of NaOH (0.2 g) in H₂O (100 mL). 2,3-Dichloro-5,6-dicyano-1,4-benzoquinone (9.6 mg, 0.042 mmol) was then added, and the resulting biphasic mixture was vigorously shaken for 2 min. The organic layer was washed with H₂O (100 mL) and brine (100 mL), and then was dried over Na₂SO₄. Removal of the solvent using a rotary evaporator afforded imidacene **1** as a blue solid (9 mg, 90%). ¹H NMR (CDCl₃): δ = 1.31 (t, 12H, CH₃CH₂CH₂), 2.02 (brs, 2H, NH), 2.50 (m, 8H, CH₃CH₂CH₂), 4.13 (t, 8H, CH₃CH₂CH₂), 9.53 (s, 4H, CH=CH); ¹³C NMR (CDCl₃): δ = 15.1, 24.9, 33.0, 113.9, 141.1, 142.2, 172.8; UV/Vis (CH₂Cl₂): λ_{max} (ε M⁻¹ cm⁻¹) =

373 (131 000), 380 (sh), 611 (49 000), 645 (59 000), 686 (77 000); fluorescence emission (CH_2Cl_2): $\lambda_{\text{excit}} = 373$, $\lambda_{\text{max}} = 689$ nm; LRMS (CI+): m/z (%): 483 (18) $[M+H]^+$, 253 (100); HRMS (CI+): calcd for $\text{C}_{28}\text{H}_{35}\text{N}_8$: 483.2985; found 483.2989. Analytical samples (violet needles), prepared by dissolving the crude product in the minimum amount of CH_2Cl_2 and chilling the solution to -20°C overnight, were consistently low in carbon.

Computational Methods

The aromatic stabilization energy (ASE) of a compound is evaluated by constructing an isodesmotic equation that contains the purported aromatic species as well as a non-aromatic reference system such as an olefin or conjugated polyene. The same number and types of chemical bonds exist on the two sides of the reaction arrow and the difference in energy is attributed to the ASE. By convention, the ASE is positive for aromatic species and negative for antiaromatic compounds.^[23] The reliability of ASEs varies and is closely coupled to the choice of reference system. The ASEs calculated herein utilize a homodesmotic equation, which is a specific type of isodesmotic equation that fulfills two specific criteria. First, there are equal numbers of carbon and nitrogen atoms in their various states of hybridization across the reaction arrow. Second, carbon and nitrogen atoms with zero, one, or two hydrogens bound to each are classified separately, and the numbers of atoms within each classification are identical in the reactants and products.^[24] Consistent with previous reports on ASEs for polycyclic molecules, the reference system is cyclic to more accurately account for hybridization changes and provide a sigma framework for electron delocalization.^[25] Figure 6 illustrates the homodesmotic equations used to evaluate the ASEs for the porphyrinoid macrocycles with global (Figure 6a) and local (Figure 6b and c) aromaticity. The globally aromatic macrocycle has three aromatic ring structures that the homodesmotic equation needs to accommodate: the bridged [18]annulene, the internal cross, and the (two) five-membered heterocyclic rings. The locally aromatic macrocycle has the (four) five-membered heterocyclic rings as well as the 22 π -electron perimeter and 18 π -electron bridged [18]annulene and internal cross (Figure 2). A prerequisite of the reference structure is it must occlude all possible aromatic pathways; those shown in Figure 6 achieve this purpose. Importantly, several alternative reference structures were investigated for the globally aromatic molecules reported in this study but

none yielded results which changed the qualitative conclusions. Molecular geometries for the ASE calculations were optimized with modest B3LYP/6-31G methods to avoid overwhelming the available computational resources, a choice which was justified by a favorable qualitative comparison of the ASEs of benzene, pyrrole and imidazole between the B3LYP/6-31G and B3LYP/6-31+G* methods.

Nucleus independent chemical shifts (NICS)^[9] were evaluated with GIAO-SCF/6-31+G* methods at B3LYP/6-31G* optimized geometries. Identical methods were applied to the analysis of global and local aromaticity in free and metal-bound porphyrins.^[20] Other work has suggested that polarization functions are necessary on both N and H in order to accurately model the hydrogen-bonding interaction.^[21] To this end, we have examined NICS with GIAO-SCF/6-31+G** at B3LYP/6-31G** geometries and have evaluated the HOMA at the same level. For the dianions, calculations with GIAO-SCF/6-31+G** at B3LYP/6-31+G** were examined. In all cases, the results did not alter the qualitative conclusions. Data for the calculated ^1H and ^{13}C chemical shifts were obtained from the NICS calculations. Previous work suggests that the methods we applied can be expected to yield accurate proton chemical shifts,^[26] and we assume a similar level of accuracy holds for the carbon shifts. In general, large negative NICS values (ca < -9) reflect aromatic rings, while less negative or positive values reflect non-aromatic or antiaromatic systems.

The harmonic oscillator model of aromaticity (HOMA) assesses the extent of aromaticity on structural grounds and is defined by Equation (1).

$$\text{HOMA} = 1 - \frac{\alpha}{n} \sum (R_{\text{opt}} - R_i)^2$$

$$= 1 - [\alpha (R_{\text{opt}} - R_{\text{av}})^2 + \frac{\alpha}{n} \sum (R_{\text{av}} - R_i)^2] = 1 - \text{EN} - \text{GEO} \quad (1)$$

It is based on the deviation of bond lengths from an optimal value, R_{opt} , that is defined, in this case, energetically. R_{opt} is the distance corresponding to the minimum energy, based on a harmonic potential, required to compress the bond to the double bond length and expand it to the single bond length. The empirical constant α is fixed to yield HOMA = 0 for the Kekule structure in which there is maximum bond alternation, and HOMA = 1 for the system in which all bonds are equal to the optimal value. R_{av} corresponds to the average bond length, while the n individual bond lengths, R_i , are calculated from the Pauling definition of bond number.^[27] Large values of EN and GEO translate into a low HOMA value and

therefore indicate a non-aromatic system. The EN term describes changes in the aromatic character due to the deviation of the average bond length from the optimal value, while the GEO term reflects changes due to bond length alternation. Structural data used in the HOMA analysis was evaluated at the B3LYP/6-31G*, B3LYP/6-31G**, and B3LYP/6-31+G** levels of theory.

Previous studies on related porphyrinoid macrocycles have clearly shown that the lack of electron correlation in the computational treatment leads to pronounced bond localization and low symmetry.^[28] In this context, the use of the density functional methods reported herein are critical to the accurate description of bond delocalization in the aromatic systems.

All quantum chemical calculations were performed with either the G94^[29] or G98^[30] program suite.

Acknowledgement

A.L.S. thanks the donors of The Petroleum Research Fund, administered by the American Chemical Society (Grant No. 33 590-B5), for partial support of this

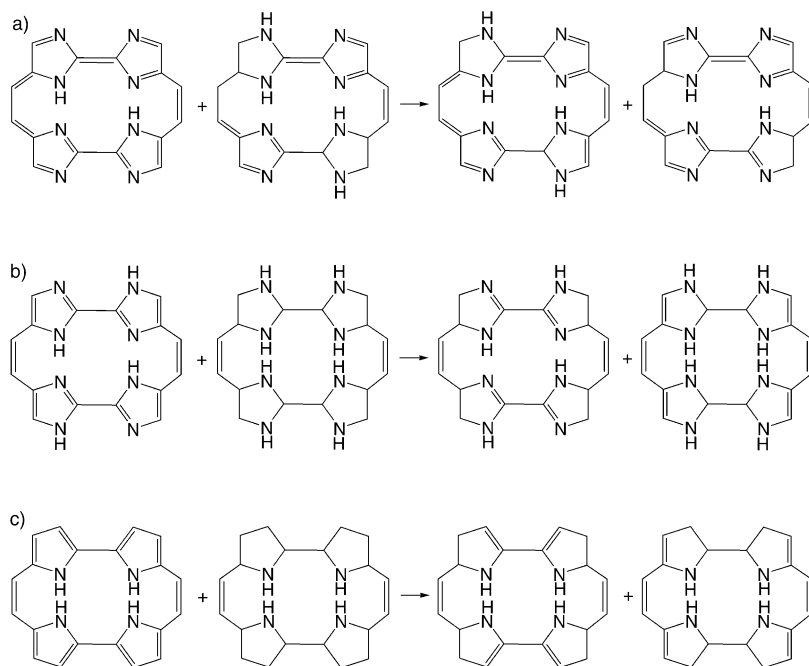


Figure 6. Homodesmotic equation for the evaluation of the aromatic stabilization energy for a) imidacene (**1**); b) dihydroimidacene (**5**); and c) dihydroporphycene (**H₂Pc**). The geometric isomer used for **H₂Pc** corresponds to that of lowest energy, adopting the orientation of rings a and a' up, b and b' down.

research. Support from the North Carolina Supercomputer Center and the ECU HPC is also acknowledged. W.E.A. thanks the Research and Creative Activity Committee of ECU for funding a portion of this work. H.L. was supported, in part, by a Burroughs-Wellcome Fellowship. The work in Austin was supported by NSF grant CHE 0107732 to J.L.S.

- [1] a) H. Furuta, H. Maeda, A. Osuka, *Chem. Commun.* **2002**, 1795–1804; b) T. D. Lash, M. J. Hayes, J. D. Spence, M. A. Muckey, G. M. Ferrence, L. F. Szczepura, *J. Org. Chem.* **2002**, *67*, 4860–4874; c) J. L. Sessler, A. Gebauer, E. Vogel, “Porphyrin Isomers,” in *The Porphyrin Handbook* (Eds.: K. M. Kadish, K. M. Smith, R. Guilard), Academic Press, San Diego, CA and Burlington, MA, **2000**; d) E. Vogel, *J. Heterocycl. Chem.* **1996**, *33*, 1461–1487; e) J. L. Sessler, E. A. Brucker, S. J. Weghorn, M. Krusters, M. Schäfer, J. Lex, E. Vogel, *Angew. Chem.* **1994**, *106*, 2402–2406; *Angew. Chem. Int. Ed. Engl.* **1994**, *33*, 2308–2312; f) E. Vogel, M. Sicken, P. Röhrig, H. Schmickler, J. Lex, O. Ermer, *Angew. Chem.* **1988**, *100*, 450–453; *Angew. Chem. Int. Ed. Engl.* **1988**, *27*, 411–414.
- [2] For recent reviews, see: a) J. L. Sessler, R. S. Zimmerman, C. Bucher, V. Král, B. Andioletti, *Pure Appl. Chem.* **2001**, *73*, 1041–1057; b) P. A. Gale, P. Anzenbacher, Jr., J. L. Sessler, *Coord. Chem. Rev.* **2000**, *222*, 57–102; c) P. A. Gale, J. L. Sessler, V. Král, *Chem. Commun.* **1998**, 1–8.
- [3] For recent reviews, see: a) J. L. Sessler, A. Gebauer, S. J. Weghorn, “Expanded Porphyrins,” in *The Porphyrin Handbook* (Eds.: K. M. Kadish, K. M. Smith, R. Guilard), Academic Press, San Diego, CA and Burlington, MA, **2000**; b) A. Jasat, D. Dolphin, *Chem. Rev.* **1997**, *97*, 2267–2340; c) J. L. Sessler, S. J. Weghorn, *Expanded, Contracted and Isomeric Porphyrins*, Elsevier, Oxford, **1997**.
- [4] a) J. Waluk, M. Müller, P. Swiderek, M. Köcher, E. Vogel, G. Hohlneicher, J. Michl, *J. Am. Chem. Soc.* **1991**, *113*, 5511–5527; b) A. Gorski, E. Vogel, J. L. Sessler, J. Waluk, *J. Phys. Chem. A* **2002**, *106*, 8139–8145; c) A. Gorski, E. Vogel, J. L. Sessler, J. Waluk, *Chem. Phys.* **2002**, *282*, 37–49.
- [5] For a recent review of aromaticity, see *Chem. Rev.* **2001**, *101*, whole Issue.
- [6] a) M. K. Cyrański, T. M. Krygowski, A. R. Katritzky, P. v. R. Schleyer, *J. Org. Chem.* **2002**, *67*, 1333–1338; b) P. v. R. Schleyer, H. Jiao, *Pure Appl. Chem.* **1996**, *68*, 209–218; c) P. George, M. Trachtman, A. M. Brett, C. W. Bock, *J. Chem. Soc. Perkin Trans. 2* **1977**, 1036–1047.
- [7] L. Pauling, J. Sherman, *J. Chem. Phys.* **1933**, *1*, 606.
- [8] J. Kruszewski, T. M. Krygowski, *Tetrahedron Lett.* **1972**, 3839–3842.
- [9] P. v. R. Schleyer, C. Maerker, A. Dransfeld, H. Jiao, N. J. R. van Eikema Hommes, *J. Am. Chem. Soc.* **1996**, *118*, 6317–6318.
- [10] E. Steiner, P. W. Fowler, L. W. Jenneskens, R. W. A. Havenith, *Eur. J. Org. Chem.* **2002**, 163–169.
- [11] T. Sternfeld, R. E. Hoffman, C. Thilgen, F. Diederich, M. Rabinovitz, *J. Am. Chem. Soc.* **2000**, *122*, 9038–9039.
- [12] A. J. Matzger, K. P. C. Vollhardt, *Tetrahedron Lett.* **1998**, *39*, 6791–6794.
- [13] E. Vogel, M. Balci, K. Pramod, P. Koch, J. Lex, O. Ermer, *Angew. Chem.* **1987**, *99*, 909–912; *Angew. Chem. Int. Ed. Engl.* **1987**, *26*, 928–931.
- [14] W. E. Allen, C. J. Fowler, V. M. Lynch, J. L. Sessler, *Chem. Eur. J.* **2001**, *7*, 721–729.
- [15] a) H. Liu, M. Sc. Thesis, East Carolina University, **2000**; b) A. L. Sargent, I. C. Hawkins, W. E. Allen, *Abstracts of Papers*, 222nd ACS National Meeting, Chicago, IL, August 26–30, **2001**, COMP-224.
- [16] a) B. W. Metcalf, F. Sondheimer, *J. Am. Chem. Soc.* **1971**, *93*, 6675–6677.
- [17] a) E. Vogel, B. Neumann, W. Klug, H. Schmickler, J. Lex, *Angew. Chem.* **1985**, *97*, 1044–1045; *Angew. Chem. Int. Ed. Engl.* **1985**, *24*, 1046–1048; b) H. Ogawa, M. Kubo, I. Tabushi, *Tetrahedron Lett.* **1973**, 361–364.
- [18] J. Michl, *Tetrahedron* **1984**, *40*, 3845–3934.
- [19] a) M. Boronat, E. Ortí, P. M. Viruela, F. Tomás, *J. Mol. Struct. Theochem* **1997**, *390*, 149–156; b) C. W. M. Kay, U. Gromadecki, J. T. Törring, S. Weber, *Mol. Phys.* **2001**, *99*, 1413–1420.
- [20] M. K. Cyrański, T. M. Krygowski, M. Wisiorowski, N. J. R. van Eikema Hommes, P. v. R. Schleyer, *Angew. Chem.* **1998**, *110*, 187–190; *Angew. Chem. Int. Ed.* **1998**, *37*, 177–180.
- [21] Y. Wu, K. W. K. Chan, C. Yip, E. Vogel, D. A. Plattner, K. A. Houk, *J. Org. Chem.* **1997**, *62*, 9240–9250.
- [22] C. Bernard, J. P. Gisselbrecht, M. Gross, E. Vogel, M. Lausmann, *Inorg. Chem.* **1994**, *33*, 2393–2401.
- [23] P. v. R. Schleyer, P. K. Freeman, H. Jiao, B. Goldfuss, *Angew. Chem.* **1995**, *107*, 332–335; *Angew. Chem. Int. Ed.* **1995**, *34*, 337–340.
- [24] a) P. George, M. Trachtman, C. W. Bock, A. M. Brett, *Theor. Chim. Acta* **1975**, *38*, 121–129; b) B. Ya. Simkin, V. I. Minkin, M. N. Glukhovtsev, *Adv. Heterocycl. Chem.* **1993**, *56*, 303–428.
- [25] M. Nendel, B. Goldfuss, K. N. Houk, K. Hafner, *J. Mol. Struct. Theochem* **1999**, *461–462*, 23–28.
- [26] B. Wang, U. Fleischer, J. F. Hinton, P. Pulay, *J. Comput. Chem.* **2001**, *22*, 1887–1895.
- [27] a) T. M. Krygowski, M. K. Cyrański, *Tetrahedron* **1996**, *52*, 1713–1722; b) T. M. Krygowski, M. K. Cyrański, *Tetrahedron* **1996**, *52*, 10255–10264; c) L. Pauling, *J. Am. Chem. Soc.* **1947**, *69*, 542–553.
- [28] K. Malsch, M. Roeb, V. Karuth, G. Hohlneicher, *Chem. Phys.* **1998**, *227*, 331–348.
- [29] *Gaussian 94*, M. J. Frisch, G. W. Trucks, H. B. Schlegel, P. M. W. Gill, B. G. Johnson, M. A. Robb, J. R. Cheeseman, T. A. Keith, G. A. Petersson, J. A. Montgomery, K. Raghavachari, M. A. Al-Laham, V. G. Zakrzewski, J. V. Ortiz, J. B. Foresman, J. Cioslowski, B. B. Stefanov, A. Nanayakkara, M. Challacombe, C. Y. Peng, P. Y. Ayala, W. Chen, M. W. Wong, J. L. Andres, E. S. Replogle, R. Gomperts, R. L. Martin, D. J. Fox, J. S. Binkley, D. J. Defrees, J. Baker, J. J. P. Stewart, M. Head-Gordon, C. Gonzalez, J. A. Pople, Gaussian, Inc., Pittsburgh, PA, **1995**.
- [30] *Gaussian 98*, M. J. Frisch, G. W. Trucks, H. B. Schlegel, G. E. Scuseria, M. A. Robb, J. R. Cheeseman, V. G. Zakrzewski, J. A. Montgomery, Jr., R. E. Stratmann, J. C. Burant, S. Dapprich, J. M. Millam, A. D. Daniels, K. N. Kudin, M. C. Strain, O. Farkas, J. Tomasi, V. Barone, M. Cossi, R. Cammi, B. Mennucci, C. Pomelli, C. Adamo, S. Clifford, J. Ochterski, G. A. Petersson, P. Y. Ayala, Q. Cui, K. Morokuma, D. K. Malick, A. D. Rabuck, K. Raghavachari, J. B. Foresman, J. Chioslowski, J. V. Ortiz, A. G. Baboul, B. B. Stefanov, G. Liu, A. Liashenko, P. Piskorz, I. Komaromi, R. Gomperts, R. L. Martin, D. J. Fox, T. Keith, M. A. Al-Laham, C. Y. Peng, A. Nanayakkara, M. Challacombe, P. M. W. Gill, P. B. Johnson, W. Chen, M. W. Wong, J. L. Andres, C. Gonzalez, M. Head-Gordon, E. S. Replogle, J. A. Pople, Gaussian, Inc., Pittsburgh, PA, **1998**.

Note added in proof: The synthesis and theoretical analysis of 2,7,12,17-tetraaryl-3,6,13,16-tetraazaporphycenes (tetraarylimidacenes) has been reported. See: S. Nonell, J. I. Borrell, S. Borrós, C. Colominas, O. Rey, N. Rubio, D. Sánchez-García, J. Teixidó, *Eur. J. Org. Chem.* **2003**, 1635–1640.

Received: December 20, 2002 [F4694]